Harnessing flow cytometry to identify discrete differences during neuronal induction of hiPSCs modeling the genetic background of Joubert syndrome

Laura Colar Zanjko[1,3], Andrea Balogh[1], Balázs Széky[1], Mária Bódi-Jakus[1], Suchitra Muenthaisong[1], Dzsenifer Kovács-Schoblocher[1], Krisztina Bánfai[1], Antonia Wiegering[2], Anita Fehér[1], Melinda Zana[1], Sylvie Schneider-Maunoury[2], András Dinnyés[1,3]

[1]BioTalentum Ltd, Aulich L u 26, 2100 Gödöllő, Hungary.
[2]Sorbonne Université, Centre National de la Recherche Scientifique (CNRS) UMR7622, Institut national pour la Santé et la Recherche Médicale U1156, Institut de Biologie Paris Seine-Laboratoire de Biologie du Développement (IBPS-LBD), 75005 Paris, France.
[3]Department of Physiology and Animal Health, Institute of Physiology and Animal Nutrition, Hungarian University of Agriculture and Life Sciences, Gödöllő, 2100, Hungary.

Medicine Made to Measure

Introduction Joubert syndrome (JS) is a neurodevelopmental ciliopathy characterized by mid-hindbrain malformation, developmental delay, hypotonia, oculomotor apraxia, and breathing disorders. Mutations in more than 35 genes encoding ciliary proteins affecting the ciliary function are associated with JS. One of these genes is RPGRIP1L encoding the retinitis pigmentosa GTPase regulator-interacting protein 1-like (RPGRIP1L) protein. RPGRIP1L is important for the primary cilium to perform various functions, such as embryonic development, neural tube formation, cilium-related sonic hedgehog signaling, cell proliferation, cell migration, cell differentiation, and apoptosis. To model the implications of the dysfunctional RPGRIP1L in the molecular pathomechanism during brain development human induced pluripotent stem cells (hiPSCs) were engineered using CRISPR/CAS9 gene editing technology to create homozygous and heterozygous gene-deletion knock-outs (KOs), and a frameshift mutant of the *RPGRIP1L* gene [1]. The hiPSCs were differentiated into neuronal stem cells (NSC) followed by neuronal and astroglial progenitor cell (NPC and APC, respectively) induction. We used flow cytometry and immunocytochemistry to monitor the expression of key markers from the start of neuronal stem cell differentiation until NPC and APC induction. The two main transcription factors involved in neurogenesis and the development of the central nervous system, Sox1 and Pax6 were downregulated in the homozygous and heterozygous KO cell lines compared to the control. As assessed by Ki67 staining, the proliferation was only slightly higher in the deletion mutant, suggesting that the RPGRIP1L deficiency does not affect cell proliferation. During the neural induction, the low PAX6 level was maintained in the full deletion-KO NPCs, whereas the RPGRIP1L+/- showed a two-fold higher expression, which was still lower than that in the WT. The A2B5 marker, expressed mainly by oligodendrocyte precursors and astroglial progenitor cells showed the lowest expression in the full deletion-KO and the frameshift mutant but was not changed in the heterozygous deletion-KO line. In conclusion, we can state that by using flow cytometry we could detect subtle quantitative and qualitative differences mirroring the genetic background differences of the modified cell lines [2].

Brain development model

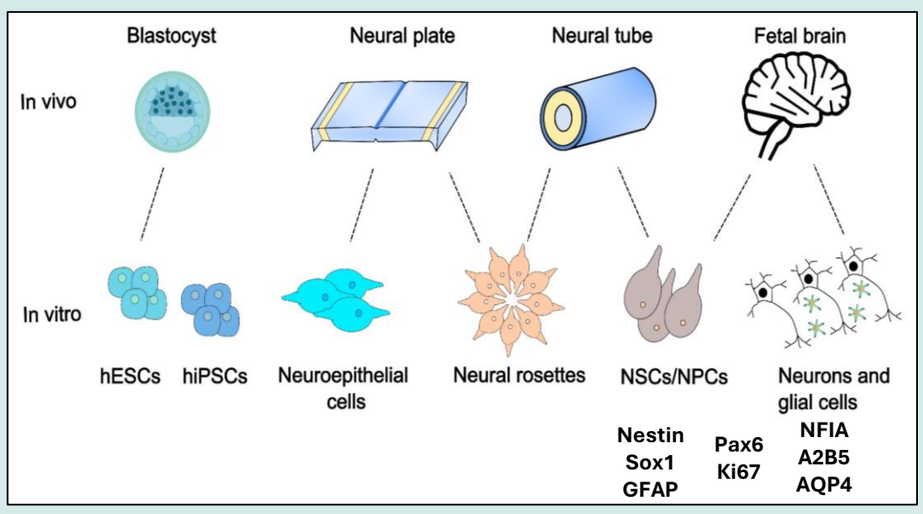

Overview of the initial stages of brain development from blastocyst to fetal brain as well as the representative *in vitro* stages with specific neural and astroglial markers present through the stages [3].

Methodology and timeline

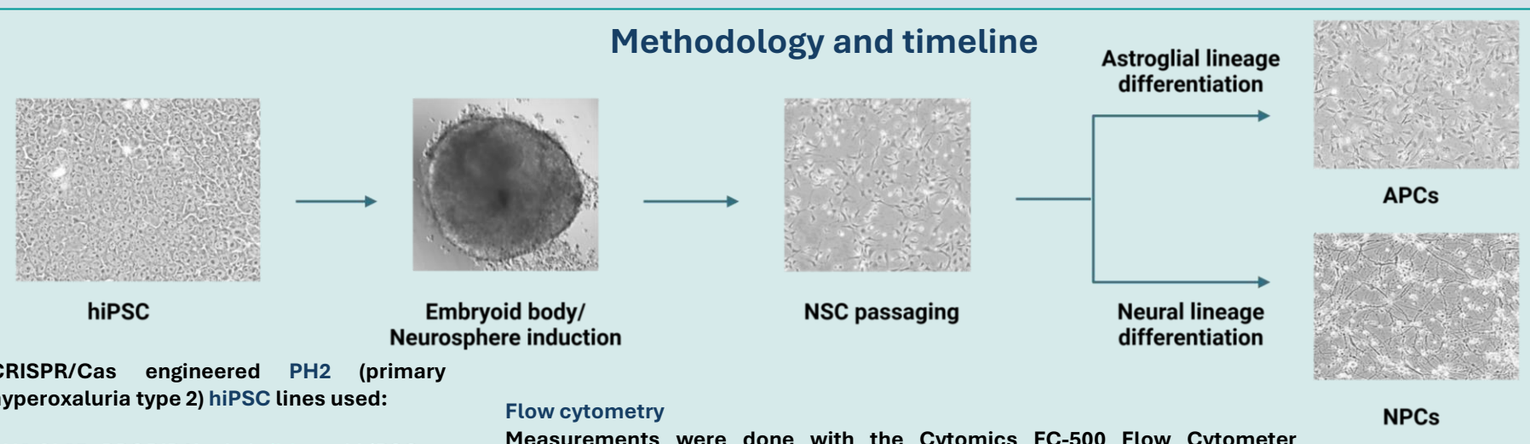

CRISPR/Cas engineered PH2 (primary hyperoxaluria type 2) hiPSC lines used:

PH2 CL25: *RPGRIP1L* +/+ (wild type) hiPSC
PH2 CL44: *RPGRIP1L* -/- (indel-KO) hiPSC
PH2 CLC5: *RPGRIP1L* -/- (homozygote deletion-KO) hiPSC
PH2 CLF6: *RPGRIP1L* +/- (heterozygote deletion-KO) hiPSC

Neural stem cells (NSCs) were induced from hiPSCs by 3D neural induction with the dual SMAD inhibition method [4].
Astrocyte progenitor cells (APCs) and neural progenitor cells (NPCs) were induced after passage 5 (P5) from the NSCs.

Flow cytometry
Measurements were done with the Cytomics FC-500 Flow Cytometer (Beckman Coulter).
The analysis was done with the FlowJo 10.0 software (BD Biosciences).
Markers were analyzed within the live cell gate after dead cell exclusion using Fixable Viability Dye eFluor™ 780 (ThermoFisher, #65-0865-14).

From P1-P4 the following conjugated antibodies were used:
Nestin Alexa Fluor 647 (BioLegend, #560393), Sox1 PE (BioLegend, #561592), pAKT Alexa Fluor 488 (R&D Systems, #IC7794G), KI67 PE (Abcam, #Ab270650), GFAP (GA5) Alexa Fluor 488 (Invitrogen, #53-9892-82), CD56 NCAM APC (BioLegend,#362503), Pax6 PE (BioLegend, #561552) and Sox9 APC (Biorbyt,#Orb1007509).
From P5 the following antibodies have been added:
AQP4 Alexa Fluor 647 (Santa Cruz Biotech, #sc-327-39) and A2B5 APC (Miltenyi, #130-123-800).

Early NSC lines present heterogenous differentiation stages diverging into two populations

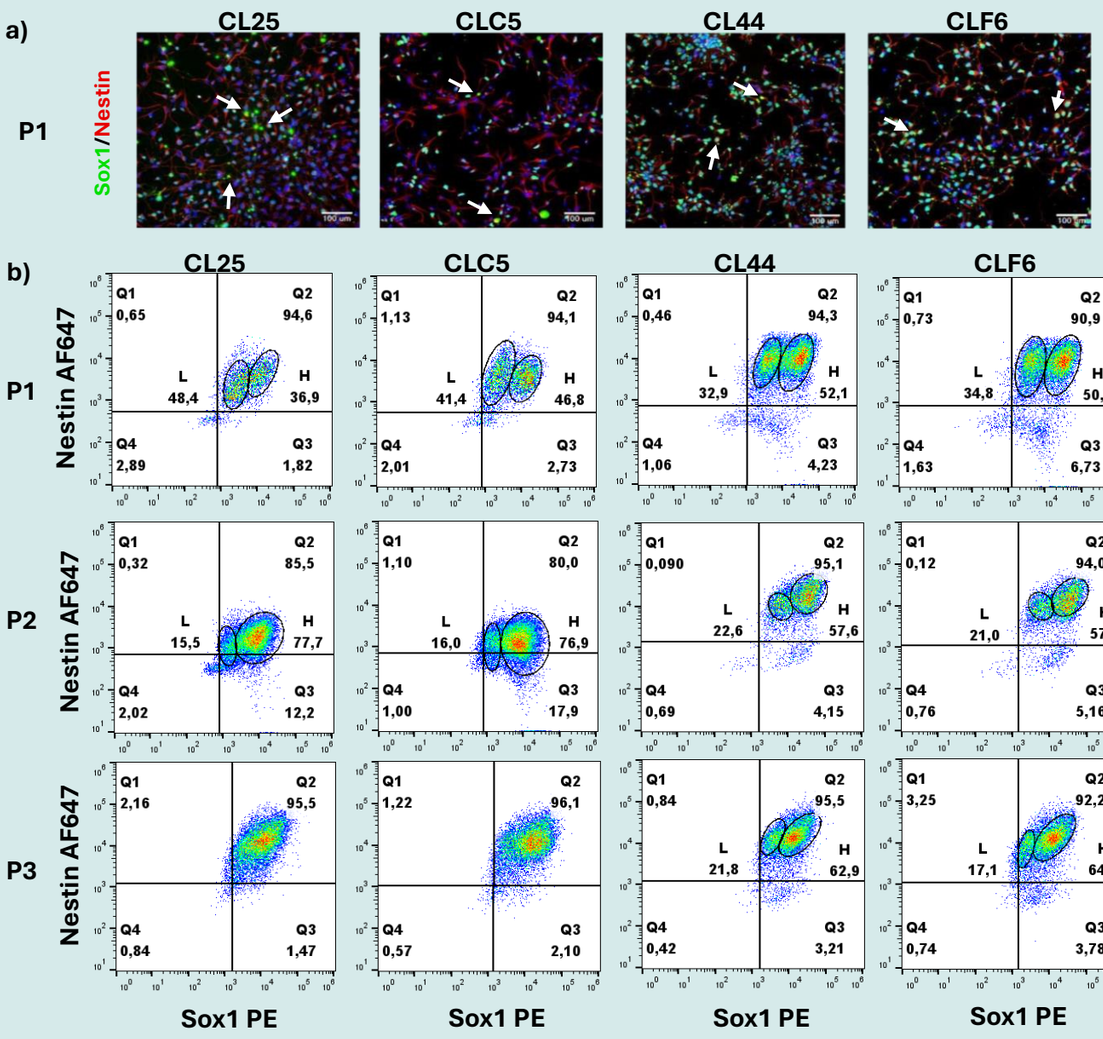

Expression of NSC markers Sox1 and Nestin in all PH2 cell lines has been confirmed through immunocytochemistry (a) and flow cytometry (b). Expression levels are not uniform in all cell lines with visibly brighter Sox1 signals in some cells (marked by arrows) in the ICC images from P1. These results have been confirmed with flow cytometry, as shown in the graphs (L-low Sox1, H-high Sox1), enabling the quantification of the signal as opposed to the ICC images. These findings confirm the presence of two populations within each cell line visible through passage 1 and 2 with a „tail" left at passage 3. Indicating that one population is further advanced in differentiation, while the other population advances rapidly and by passage 3 most cells are in the same differentiation stage.

High Nestin expression in mature NSCs reduced after APC and NPC induction

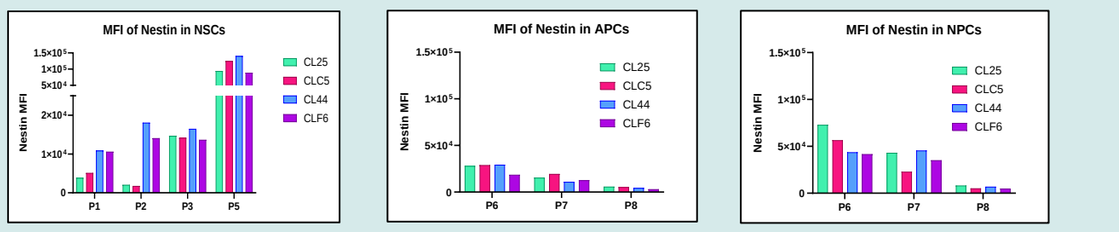

The mean fluorescence intensity (MFI) of Nestin has increased with each passage of the NSCs reaching a 15-fold increase from the initial MFI. After APC and NPC induction the MFI decrease is rapid and continues slowly through each passage, but less steep in NPCs (a). Comparing corresponding APC and NPC lines from P6 to P8 the expression of Nestin is higher in all NPC lines (b).

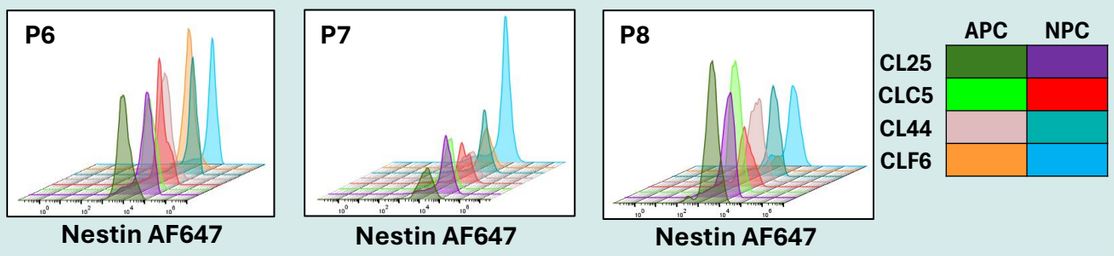

Conclusions Flow cytometry presents as a viable method to analyse neural and astroglial cultures, being able to detect subtle variations between different mutants at the NSC, APC and NPC stage of development. These minor differences can aid the understanding of the effect of specific genetic mutations on the phenotype of neuronal cultures, therefore helping in establishing relevant disease models.

Pax6 expression is decreased in CLC5 mutant during the NSC maturation continuing after NPC and APC induction. Opposite to Pax6 expression Ki67 is increased in CLC5 mutant

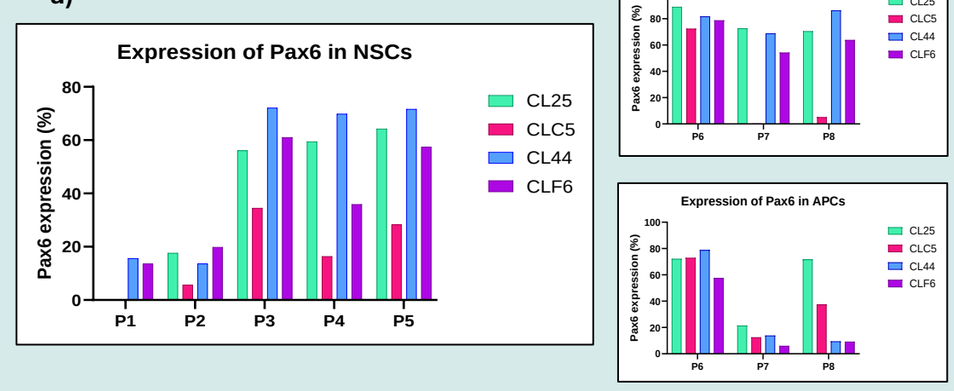

Pax6 expression increases as NSCs mature except the CLC5 mutant. In APCs Pax 6 expression rapidly drops at P7, while it stagnates in NPCs, except the CLC5 mutant (a).
At P3 of the NSCs a negative correlation is present as the CLC5 mutant has the lowest Pax6 expression and the highest Ki67 expression, confirming the CLC5 mutant is less differentiated than the *wt* and other mutants (b).

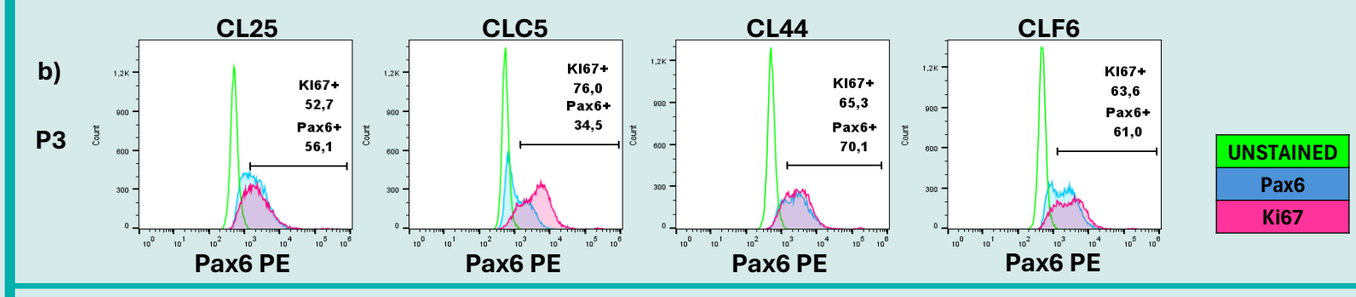

Heterogenous differentiation stages persist in APCs and NPCs based on Ki67 expression

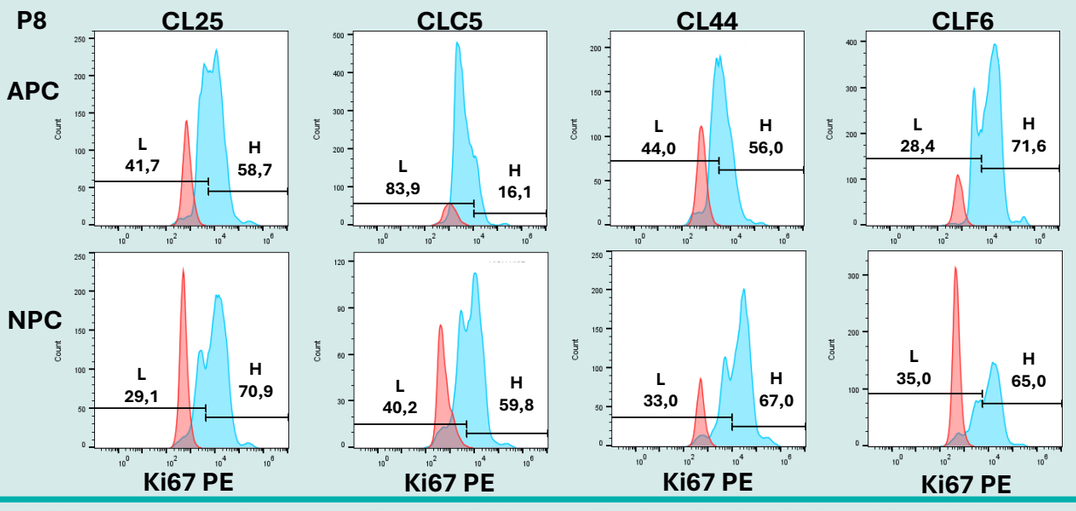

Expression levels of Ki67 in P8 reveal the presence of two populations with different expression levels in each APC and NPC cell line (L-low Ki67, H-high Ki67). Populations with a higher Ki67 expression are highly proliferative. Similar to Sox1 in NSCs, this confirms heterogeneous differentiation in all APC and NPC lines.

A2B5 expression confirms differentiation is inhibited in CLC5 and CL44 mutants

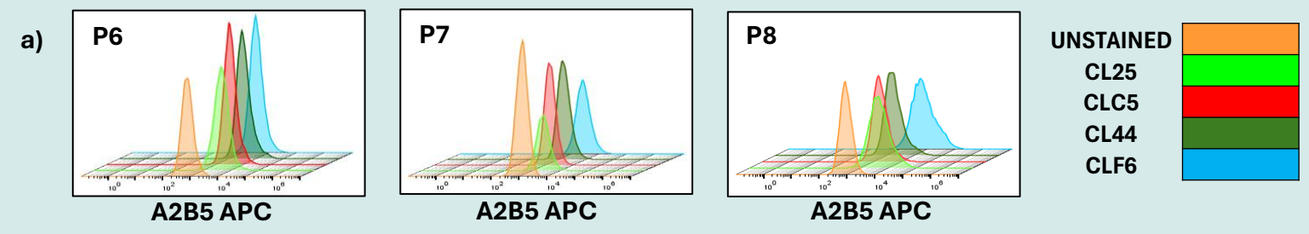

A2B5 expression correlates with Pax6 expression (section above) peaking at P6 and decreasing rapidly at P7 with a low spike at P8 (a). Levels of GFAP remained high through all passages, while AQP4 has a lower expression in CLC5 and CL44 mutants (b). These glial markers show a lower level of differentiation in the *knock-out* mutants.

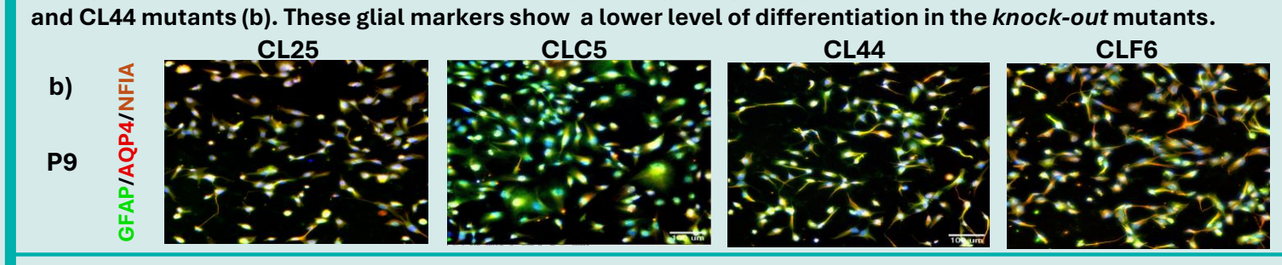

Acknowledgements This study was supported by ERA-NET NEURON Research Programme (No. 2019-2.1.7-ERA- NET-2022-00031, NDCil), by Med4Cure /Cardiabetter IPCEI from the Hungarian Ministry for National Economy, the Hungarian Grant No. 2020–1.1.5-GYORSÍTÓSÁV-2021-00016 from the National Research, Development and Innovation Fund and by the Medicine to Measure project (No. HORIZON-MSCA-2022-DN-01-01) from the MARIE SKŁODOWSKA-CURIE ACTIONS Doctoral Networks (DN).

References [1]: Wiegering, A., Dildrop, R., Vesque, C., Khanna, H., Schneider-Maunoury, S., & Gerhardt, C. (2021). Rpgrip1l controls ciliary gating by ensuring the proper amount of Cep290 at the vertebrate transition zone. Molecular biology of the cell, 32(8), 675–689. [2]: Wiegering A., Isabelle Anselme, Brunetti L.,Metayer-Derout L., Calderon D., Thomas S., Nedelec S., Eschstruth A., Serpieri V., Catala M., Antoniewski C., Schneider-Maunoury, S., & Stedman, A., A differential requirement for ciliary transition zone proteins in human and mouse neural progenitor fate specification, bioRxiv 2024.02.28.582477. [3] : Horánszky, A. (2024). Human-induced pluripotent stem cell-derived in vitro neural models for the investigation of environmental alterations on embryonic brain development. 29. [4] : Chambers, S. M., Fasano, C. A., Papapetrou, E. P., Tomishima, M., Sadelain, M., & Studer, L. (2009). Highly efficient neural conversion of human ES and iPS cells by dual inhibition of SMAD signaling. Nature biotechnology, 27(3), 275–280